Academic Journal of Science and Technology
ISSN: 2771-3032 | Vol. 13, No. 1, 2024

Dark Matter Interpretation of the Fermi-LAT Galactic Center Excess

Alan Lu

Saratoga High School, Saratoga, 95070, USA

Abstract: In this work, we analyze the γ-ray Galactic Center Excess (GCE) as a potential signal from dark matter (DM) annihilation. Using updated annihilation spectra, we calculate the gammaray flux for various annihilation channels and compare the results to those obtained from previous analyses of Fermi-LAT data. We assume generalized Navarro-Frenk-White (gNFW) and Einasto DM density profiles, from which we estimate the geometrical factor $\bar{J}$. We determine the best-fit DM mass and annihilation cross section for each channel, with the *b* quark, *Z* boson, and *W* boson channels yielding the most favorable results. The *b* quark channel provides a good match with a DM mass around 45–60 GeV and a cross section near the thermal relic value. These findings reinforce the viability of the DM annihilation scenario for the GCE, and we present spectra and cross section comparisons that strengthen this interpretation.

Keywords: Galactic Center Excess (GCE); dark matter (DM); Fermi-LAT.

1. Introduction

Several observations of astrophysical objects at different scales point to the existence of DM in the universe. These observations include the rotational curves of galaxies, gravitational lensing, the cosmic microwave background, and the large-scale structure of the universe [3,5]. In spiral galaxies, for example, the outer regions rotate much faster than can be explained by the visible matter alone, suggesting the presence of DM providing additional gravitational pull [1–3]. Similarly, gravitational lensing, where light from distant objects is bent by a massive foreground object, reveals that only a few percent of matter is visible in galaxies and galaxy clusters. The cosmic microwave background radiation also shows fluctuations that can only be accounted for with a significant amount of DM influencing the early universe's structure formation. Moreover, simulations of galaxy formation and evolution only match observations when DM is included. Collectively, these observations suggest that DM is the dominant matter component of the universe, making up about 85% of its total mass. Moreover, if DM is made of new particles with respect to the Standard Model, it should be weakly interacting, stable on cosmological scales, and cold (i.e. nonrelativistic in the current universe) [5–7].

Indirect detection strategies for DM particles are among the most promising approaches within DM search. These methods involve searching for the products of DM particle interactions rather than detecting DM particles directly, such as gamma rays, neutrinos, antiprotons, or positrons [8]. One of the main focuses within indirect detection is detecting excess secondary particle emissions from the galaxy, which cannot be attributed to known astrophysical sources. Among the rarest cosmic particles used for indirect detection, gamma rays are among the most promising one because they travel straight in the Universe without being deflected by magnetic fields. Therefore, gamma rays can be used to search for DM signals from astrophysical objects with the predicted highest density. The Galactic center, in particular, is the direction of the sky where we would expect the largest flux.

The Fermi Large Area Telescope (Fermi-LAT) provides pivotal observations in indirect detection research [13]. This telescope is designed to observe gamma rays in the energy range from 20 MeV to over 1000 GeV. Several groups have searched for a possible DM signal in the direction of the Galactic Center, finding indeed a very significant excess known as the Galactic Center Excess (GCE). However, its exact characteristics are affected by the choice of the interstellar emission (IEM). In fact, around 90-95% of the gamma-ray emissions can be explained by the IEM. The IEM primarily accounts for interactions between cosmic rays and the interstellar medium, including processes like inverse Compton scattering and gamma-ray production from neutral pion decay. The other two important components of the gamma-ray data are resolved sources and an isotropic emission, which is due to the cumulative flux of faint sources [15]. The origin of the GCE is still debated. Initially, the GCE was considered a potential signal of DM annihilation, as its spectrum, angular distribution, and intensity aligned with predictions for DM particles. Analysis using various IEM templates consistently exhibits that the GCE spectrum (measured in E^2dN/dE) peaks at a few GeV, predicts a spherically symmetric DM halo, and is well centered in the Galactic Center [11,21].

Over time, alternative explanations for GCE have emerged. Some studies proposed unresolved astrophysical sources, like millisecond pulsars, as the cause, citing spatial clustering of gamma rays and a distribution aligned with the Galactic Bulge [9,10]. However, new analyses weaken the evidence for the existence of a pulsar bulge and thus reaffirm the DM hypothesis. [12] showed that photon clustering was an artifact of background misinterpretation. Refined models indicate the GCE lacks significant small-scale power, contradicting a pulsar explanation [23]. These findings, along with excess antiprotons observed by the Alpha Magnetic Spectrometer, support DM annihilation as the source of the GCE [22].

Significant uncertainties still remain about the nature of the DM interpretation, particularly in regard to the GCE. In this paper, we address these uncertainties by providing new estimations of the geometrical factor $\bar{J}$ which describes the line-of-sight integral of the squared DM density, based on the work in [19]. Building on these estimations, we use the latest theoretical DM annihilation source spectra in Arina et al.

(2023) [18], which account for a wide range of DM masses and final states, including the production of Standard Model fermions and bosons. For each annihilation channel, we calculate the expected gamma-ray energy spectra, represented as E^2dN/dE, and directly compare them to observed data from the Fermi-LAT, using results from two recent independent studies: di Mauro (2021) [15] and Cholis et al. (2022) [16]. In particular, we conduct a detailed analysis, estimating the best-fit DM mass and annihilation cross section for each annihilation channel. Additionally, we compare our findings to the thermal relic cross section presented in Bringmann et al. (2021) [20] to evaluate how closely our results align with theoretical predictions of DM annihilation rates.

2. Gamma Ray Flux from DM Annihilation

We focus on the high energy gamma rays produced from prompt (direct) emission. Secondary production of gamma rays coming from inverse Compton scattering can contribute significantly only below 1 GeV where the GCE is detected with low significance. We consider DM particles annihilating into final state f (fermions or gauge bosons of the Standard Model) $\chi+\chi \rightarrow f\bar{f}$. The differential photon flux of this process is given by

$$\frac{dN}{dE} = \frac{1}{2}\frac{r_\odot}{4\pi}\left(\frac{\rho_\odot}{M_{DM}}\right)^2 \bar{\mathcal{J}}\langle\sigma v\rangle_f \frac{dN_\gamma^f}{dE}, \quad (1)$$

where $r\odot$ is the distance to the Galactic Center, $\rho\odot$ is the local DM density at the Sun, M_{DM} is the DM mass, $\langle\sigma v\rangle_f$ is the averaged annihilation cross-section, dN_γ^f/dE is the differential gamma-ray spectrum, and $\bar{J}$ is the geometrical factor averaged over a solid angle $\Delta\Omega$ [14,17].

For dN_γ^f/dE, we use the recently derived annihilation source spectra calculated by Arina et al (2023) [18], which cover a wide range of DM masses (5 GeV to 100 TeV) and annihilation channels. These updated spectra account for complex interactions such as the emission of massive gauge bosons for precision.

2.1. Estimation of the geometrical factor

The average geometrical factor $\bar{J}$ is the line of sight (l.o.s.) s integral of the squared DM density distribution averaged over a viewing angle $\Delta\Omega$, given as

$$\bar{\mathcal{J}} = \frac{1}{\Delta\Omega}\int_{\Delta\Omega} d\Omega \int_{\text{l.o.s.}} \frac{ds}{r_\odot}\left(\frac{\rho(r(s,\theta))}{\rho_\odot}\right)^2, \quad (2)$$

where $r(s,\theta) = (r_\odot^2 + s^2 - 2r_\odot s\cos\theta)^{1/2}$ is the radius measured from the galactic center [14,17].

Following the work in [15, 16], we consider the rectangular region of the sky with longitudes $b_{\min} = 0^\circ$, $b_{\max} = 20^\circ$ and latitudes $l_{\min} = 2^\circ$, $l_{\max} = 20^\circ$. We focus on this region since the GCE is more pronounced here, accounting for up to $O(10\%)$ of the total emission. Thus, we may calculate the solid angle and geometrical factor as

$$\Delta\Omega = 4\int_{b_{\min}}^{b_{\max}}\int_{\ell_{\min}}^{\ell_{\max}} db\, d\ell\, \cos b, \quad \bar{\mathcal{J}} = \frac{4}{\Delta\Omega}\int\int db\, d\ell\, \cos b\, J(\theta(b,\ell)) \quad (3)$$

For our viewing region, we find the solid angle $\Delta\Omega = 0.429$ steradians.

The specific calculation of $J(\theta(b,l))$ depends on the specific profile used for the DM halo to calculate $\rho(r)$. We consider two widely used profiles:

The generalized Navarro-Frenk-White (gNFW) profile, given as

$$\rho_{\text{gNFW}}(r) = \frac{\rho_0}{\left(\frac{r}{r_s}\right)^\gamma\left(1+\frac{r}{r_s}\right)^{3-\gamma}},$$

where ρ_0 is the normalization constant, r_s is the scale radius, and γ is the slope parameter varying in the range 0-2. $\gamma = 1$ corresponds to the original NFW profile. Larger γ lead to steeper inner profiles.

The Einasto profile, given as

$$\rho_{\text{Ein}}(r) = \rho_0 \exp\left(-\frac{2}{\alpha}\left[\left(\frac{r}{r_s}\right)-1\right]\right),$$

where α is the slope parameter varying in the range 0-1. Compared to the gNFW profile, the Einasto profile is typically less steep for larger radii.

The analysis in [19] examined the Milky Way's rotation curves to model its DM distribution by fitting the NFW, gNFW, and Einasto profiles to their baryonic models. We use three benchmark cases in the baryonic model B1, which has slope parameters of $\gamma = 1$, $\gamma = 1.2$, and $\alpha = 0.11$ respectively. This choice permits us to bracket the uncertainties related to the distribution of DM in the center of the Galaxy. In particular, we find geometrical factor values of 53.8, 97.2, and 116.8 respectively.

3. Results

We report the best-fit DM mass and cross section for several annihilation channels, using the results for the GCE flux obtained from [15,16]. We show the best-fit values for the DM mass and annihilation cross section found when assuming the median value of the geometrical factor $\bar{J}$. However, we can obtain the uncertainties due to the knowledge of the geometrical factor by simply rescaling the best-fit of the annihilation cross section $\langle\sigma v\rangle$ by the variation of J between the minimum and the maximum. In particular, we can apply rescaling factors of $J_{min}/\bar{J} = 53.8/97.2 = 0.55$ to $J_{max}/\bar{J} = 116.8/97.2 = 1.20$.

In the analysis we fit the flux of gamma rays from DM to the data from [15,16]. With two free parameters of DM mass and cross section, we calculate the reduced chi-squared value as:

$$\chi^2_\nu = \frac{\chi^2}{\nu} = \frac{\chi^2}{N_{data}-2},$$

where N_{data} is the number of data points, v is the number of degrees of freedom defined as $N_{\text{data}}-2$, where two refers to the number of free parameters in the model. For [15], $N_{\text{data}} = 23$, giving $\chi^2_\nu = \chi^2/21$. For [16], $N_{\text{data}} = 14$, giving $\chi^2_\nu = \chi^2/12$. The results of the parameters are reported in Table 1.

Table 1. Best fits for the DM mass and annihilation cross section obtained when fitting the data for the GCE reported in [15] (left) and [16] (right).

Channel	M_{DM} (GeV)	$\langle\sigma v\rangle$ (cm^{3}s^{-1})	χ^2_ν
$b\bar{b}$	45.6	$3.41 \cdot 10^{-26}$	0.76
$u\bar{u}$	19.6	$1.37 \cdot 10^{-26}$	1.09
$d\bar{d}$	21.6	$1.53 \cdot 10^{-26}$	1.07
$c\bar{c}$	31.5	$2.34 \cdot 10^{-26}$	0.93
$s\bar{s}$	31.0	$1.79 \cdot 10^{-26}$	1.05
e^+e^-	22.8	$2.59 \cdot 10^{-26}$	5.30
$\mu^+\mu^-$	20.0	$5.98 \cdot 10^{-26}$	5.14
$\tau^+\tau^-$	20.0	$1.16 \cdot 10^{-26}$	3.17
ZZ	38.3	$3.25 \cdot 10^{-26}$	0.72
W^+W^-	36.0	$2.94 \cdot 10^{-26}$	0.79

Channel	M_{DM} (GeV)	$\langle\sigma v\rangle$ (cm^{3}s^{-1})	χ^2_ν
$b\bar{b}$	61.4	$3.03 \cdot 10^{-26}$	1.13
$u\bar{u}$	32.2	$1.51 \cdot 10^{-26}$	1.21
$d\bar{d}$	32.9	$1.53 \cdot 10^{-26}$	1.25
$c\bar{c}$	46.0	$2.09 \cdot 10^{-26}$	1.26
$s\bar{s}$	40.6	$2.04 \cdot 10^{-26}$	1.38
e^+e^-	10.0	$3.15 \cdot 10^{-26}$	7.87
$\mu^+\mu^-$	10.0	$6.46 \cdot 10^{-26}$	7.88
$\tau^+\tau^-$	11.14	$8.17 \cdot 10^{-27}$	3.17
ZZ	58.6	$4.01 \cdot 10^{-26}$	0.87
W^+W^-	46.9	$3.14 \cdot 10^{-26}$	1.09

As shown above, the lowest chi-square values are obtained with the $b\bar{b}$ quarks, the ZZ and W^+W^- boson channels. Also, the other quark channels provide reasonable fits with reduced chi-square of the order of 1. However, the calculated DM masses for the ZZ and W^+W^- channels, are around 40–50 GeV. This means that the produced bosons should be significantly offshell with respect to the on-shell boson masses of 91.2 GeV and 80.4 GeV, respectively. Most of the DM model assuming a specific particle physics theory predict that the branching ratio into the W^+W^- and ZZ channels are highly suppressed the more the bosons are offshell. Even when accounting for the boson decay widths (approximately 2 GeV), the inferred DM masses remain unrealistically low. Nonetheless, the $b\bar{b}$ quark channel offers a more consistent and reliable fit with the data, making it a stronger candidate for explaining the GCE.

Instead, the leptonic channels do not provide a good fit to the GCE data. In fact, for both the [15,16] dataset we obtain reduced chi-square larger than 1. We should mention that we are not including inverse Compton scattering that might play a role in flux for energies below 1 GeV. However, at these energies the GCE spectrum us very uncertain.

We provide the energy spectra graphs of the $b\bar{b}$ channel below. As shown, the DM model fits well in both cases, especially for the dataset in [15]. This DM channel fits the entire energy range, even in the higher-energy tail. However, we note that the best fit to the Cholis data is significantly lower than the data above 10 GeV. The steep drop off contributes to a slight degradation in the fit quality for the [16] model compared to [15]. Nevertheless, the fit in both cases provides strong support for the DM interpretation in the b channel.

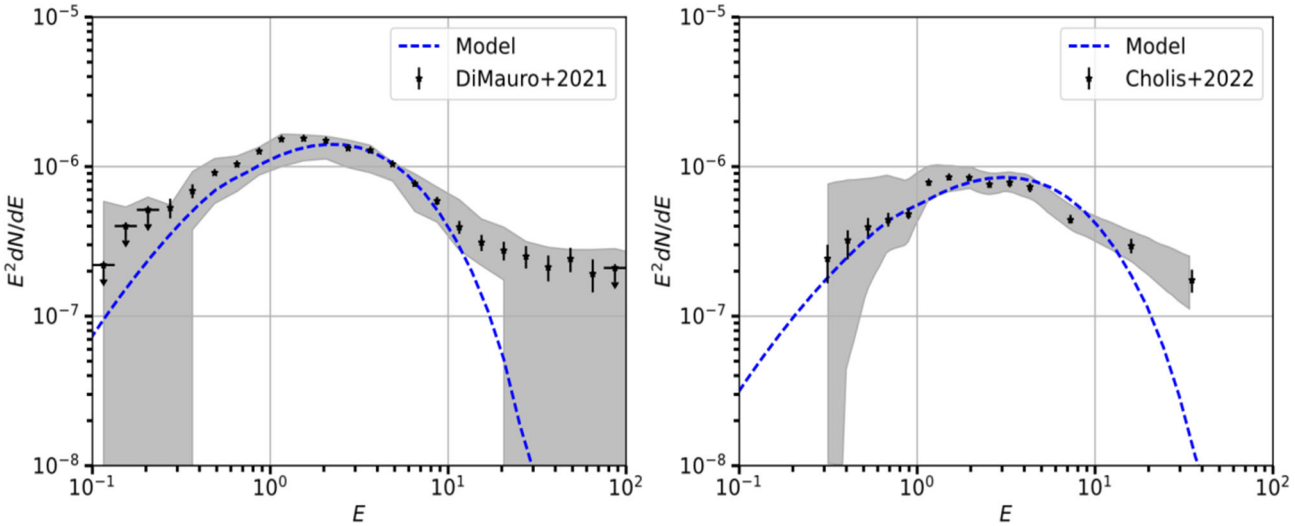

Figure 1. We show in this figure the fit obtained with DM and the $b\bar{b}$ channel to the GCE data from [15] (left) and [16] (right).

Lastly, we compare the values of the thermal cross section calculated by Bringmann et al. (2021) [20] to our results for the $\langle\sigma v\rangle$. As shown in Figure 2, the $b\bar{b}$ channel overall aligns with the predicted thermal cross section for Majorana particles (green). We also include in the same figure the FermiLAT upper limit obtained with a combined analysis of Milky Way dwarf-spheroidal galaxies for the $b\bar{b}$ (black) and $\tau\bar{\tau}$ channels (red).

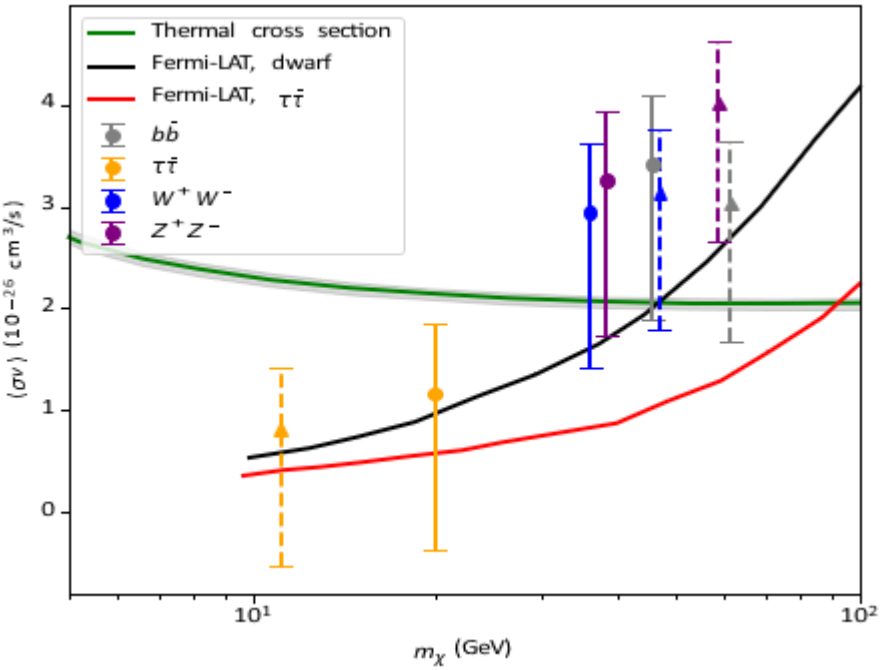

Figure 2. Thermal cross section graph. Solid lines are di Mauro (2021) and dotted lines are Cholis et al. (2022).

4. Conclusion

In this study, we investigated the DM interpretation of the Galactic Center Excess (GCE) by analyzing the γ-ray energy spectra from DM annihilation. We focused on prompt γ-ray emissions in various annihilation channels using updated annihilation spectra from [18] and compared our results to Fermi-LAT observations from [15] and [16]. We calculated the best-fit DM masses and annihilation cross sections for a range of final states, using a median value of the geometrical factor $\bar{J}$ based on the gNFW profile with a slope parameter of $\gamma = 1.2$.

Our results demonstrate that the $b\bar{b}$ quarks, the ZZ and W^+W^- boson annihilation channels provided the best fits, with masses around 45–60 GeV and cross sections near the thermal relic value of $\langle\sigma v\rangle \sim 3 \times 10^{-26}$ cm^{3}s^{-1}. However, we found that the inferred DM masses for the Z and W boson channels were significantly lower than the masses of these bosons, suggesting that these channels are less likely to be responsible for the GCE. All the quark channels, except for the top one, provide a reasonable fit, consistent with expectations for cold DM models.

Our comparison with the thermal cross section reported [20] suggests that the DM annihilation interpretation is viable within the uncertainties of the annihilation cross section and DM halo profile. However, the uncertainty within the geometrical factor makes it difficult to make precise predictions on the $\langle\sigma v\rangle$. Thus, significant uncertainties remain regarding the nature of the GCE. Alternative explanations such as unresolved astrophysical sources (e.g., millisecond pulsars) cannot be completely eliminated.

In future work, further refinement of the gamma-ray background models and improved sensitivity of indirect detection methods will be essential to narrowing down the possible DM contributions to the GCE. Observations from other sources or detection methods could provide additional evidence to confirm or refute the DM annihilation hypothesis.

References

[1] Rubin, V. C., Ford, W. K., Jr., & Thonnard, N. (1980). Rotational properties of 21 Sc galaxies with a large range of luminosities and radii, from NGC 4605 (R=4 kpc) to UGC 2885 (R=122 kpc). Astrophysical Journal, 238, 471–487. https://doi.org/10.1086/158003

[2] Hoeneisen, B. (2019). A study of dark matter with spiral galaxy rotation curves. International Journal of Astronomy and Astrophysics, 9(2), 71-96. https://doi.org/10.4236/ijaa.2019.92007

[3] Persic, M., & Salucci, P. (1996). The universal galaxy rotation curve. Monthly Notices of the Royal Astronomical Society, 281(1), 27-47. https://doi.org/10.1093/mnras/281.1.27

[4] Goodenough, L., & Hooper, D. (2009). Possible evidence for dark matter annihilation in the inner Milky Way from the Fermi Gamma Ray Space Telescope. arXiv. Fermi National Accelerator Laboratory. https://doi.org/10.48550/arXiv.0910.2998

[5] Bertone, G., Hooper, D., & Silk, J. (2004). Particle Dark Matter: Evidence, Candidates and Constraints. arXiv. https://doi.org/10.48550/arXiv.hep-ph/0404175

[6] Peebles, P. J. E. (1982). Large-scale background temperature and mass fluctuations due to scale-invariant primeval perturbations. Astrophysical Journal, Part 2 - Letters to the Editor, 263(L1-L5). https://doi.org/10.1086/183911

[7] Steigman, G., Dasgupta, B., & Beacom, J. F. (2012). Precise relic WIMP abundance and its impact on searches for dark matter annihilation. Physical Review D, 86(023506). https://doi.org/10.1103/PhysRevD.86.023506

[8] Hooper, D. (2019). TASI lectures on indirect searches for dark matter. Proceedings of Science, 333, 010. https://doi.org/10.22323/1.333.0010

[9] Bartels, R., Krishnamurthy, S., & Weniger, C. (2016). Strong support for the millisecond pulsar origin of the Galactic Center GeV excess. Physical Review Letters, 116(5), 051102. https://doi.org/10.1103/PhysRevLett.116.051102

[10] Lee, S. K., Lisanti, M., Safdi, B. R., Slatyer, T. R., & Xue, W. (2016). Evidence for unresolved γ-ray point sources in the

Inner Galaxy. Physical Review Letters, 116(5), 051103. https://doi. org/10.1103/PhysRevLett.116.051103

[11] Calore, F., Cholis, I., & Weniger, C. (2015). Background model systematics for the Fermi GeV excess. Journal of Cosmology and Astroparticle Physics, 2015(03), 038. https://doi.org/10. 1088/1475-7516/2015/03/038

[12] Leane, R. K., & Slatyer, T. R. (2019). Revival of the dark matter hypothesis for the Galactic Center gamma-ray excess. Physical Review Letters, 123(24), 241101. https://doi.org/10. 1103/PhysRevLett.123.241101

[13] Atwood, W. B., Abdo, A. A., Ackermann, M., Althouse, W., Anderson, B., Axelsson, M., Baldini, L., Ballet, J., Band, D. L., Barbiellini, G., Bartelt, J., Bastieri, D., Baughman, B. M.,Bechtol, K., B´ed´er`ede, D., Bellardi, F., Bellazzini, R., Berenji, B., Bignami, G. F., ...Ziegler, M. (2009). The Large Area Telescope on the Fermi Gamma-Ray Space Telescope mission. The Astrophysical Journal, 697(2), 1071-1102. https://doi.org/10.1088/0004-637X/697/2/1071

[14] Cirelli, M., Corcella, G., Hektor, A., Hu¨tsi, G., Kadastik, M., Panci, P., Sala, F., Strumia, A., & Tempel, E. (2012). PPPC 4 DM ID: A poor particle physicist cookbook for dark matter indirect detection. arXiv. https://doi.org/10.48550/arXiv.1012.4515

[15] Di Mauro, M. (2021). The characteristics of the Galactic center excess measured with 11 years of Fermi-LAT data. arXiv. https://doi.org/10.48550/arXiv.2101.04694

[16] Cholis, I., Zhong, Y.-M., McDermott, S. D., & Surdutovich, J. P. (2022). The return of the templates: Revisiting the Galactic Center Excess with multi-messenger observations. arXiv. https://doi.org/10.48550/arXiv.2112.09706

[17] Di Mauro, M., & Wolfgang Winkler, M. (2021). Multimessenger constraints on the dark matter interpretation of the Fermi-LAT Galactic center excess. arXiv. https://doi.org/10.48550/ arXiv.2101.11027

[18] Arina, C., Di Mauro, M., Fornengo, N., Heisig, J., Jueid, A., & Ruiz de Austri, R. (2023). CosmiXs: Cosmic messenger spectra for indirect dark matter searches. arXiv. https://doi.org/10.48550/arXiv.2312.01153

[19] de Salas, P. F., Malhan, K., Freese, K., Hattori, K., & Valluri, M. (2019). On the estimation of the local dark matter density using the rotation curve of the Milky Way. arXiv. https: //doi.org/10.48550/arXiv.1906.06133

[20] Bringmann, T., Depta, P. F., Hufnagel, M., & Schmidt-Hoberg, K. (2021). Precise dark matter relic abundance in decoupled sectors. arXiv. https://doi.org/10.48550/arXiv.2007.03696

[21] Daylan, T., Finkbeiner, D. P., Hooper, D., Linden, T., Portillo, S. K. N., Rodd, N. L., & Slatyer, T. R. (2016). The characterization of the gamma-ray signal from the central Milky Way: A case for annihilating dark matter. Physics of the Dark Universe, 12, 1-23. https: //doi.org/10.1016/j.dark.2016.02.002

[22] Aguilar, M., Ali Cavasonza, L., Ambrosi, G., Arruda, L., Attig, N., Aupetit, S., Bar˜ao, F., Barrin, L., Bartoloni, A., Ba¸se˘gmez-du Pree, S., Bates, J., Battiston, R., Behlmann, M., Beischer, B., Berdugo, J., Bertucci, B., Bindi, V., de Boer, W., Bollweg, K., & Borgia, B., et al. (2021). The Alpha Magnetic Spectrometer (AMS) on the international space station: Part II — Results from the first seven years. Physics Reports, 894(1), 1-116.

[23] Zhong, Y.-M., McDermott, S. D., Cholis, I., & Fox, P. J. (2020). Testing the sensitivity of the Galactic Center excess to the point source mask. Physical Review Letters, 124(23), 231103.https://doi.org/10.1103/PhysRevLett.124.231103